Photooxidation of cytochrome P450-BM3

Maraia E. Ener[a], Young-Tae Lee[b], Jay R. Winkler[a], Harry B. Gray[a,1], and Lionel Cheruzel[a,1,2]

[a]Beckman Institute, California Institute of Technology, 1200 East California Boulevard, Pasadena, CA 91125; and [b]The Scripps Research Institute, 10550 North Torrey Pines Road, La Jolla, CA 92037

High-valent iron-oxo species are thought to be intermediates in the catalytic cycles of oxygenases and peroxidases. An attractive route to these iron-oxo intermediates involves laser flash-quench oxidation of ferric hemes, as demonstrated by our work on the ferryl (compound II) and ferryl porphyrin radical cation (compound I) intermediates of horseradish peroxidase. Extension of this work to include cytochrome P450-BM3 (CYP102A1) has required covalent attachment of a Ru^{II} photosensitizer to a nonnative cysteine near the heme (Ru^{II}_{K97C}-Fe^{III}_{P450}), in order to promote electron transfer from the Fe^{III} porphyrin to photogenerated Ru^{III}. The Ru^{II}_{K97C}-Fe^{III}_{P450} conjugate was structurally characterized by X-ray crystallography (2.4 Å resolution; Ru-Fe distance, 24 Å). Flash-quench oxidation of the ferric-aquo heme produces an Fe^{IV}-hydroxide species (compound II) within 2 ms. Difference spectra for three singly oxidized P450-BM3 intermediates were obtained from kinetics modeling of the transient absorption data in combination with generalized singular value decomposition analysis and multiexponential fitting.

ruthenium bipyridine | enzyme catalysis

The cytochromes P450 constitute a superfamily of thiolate-ligated heme enzymes so named because the Soret absorption band in their CO-bound derivatives peaks near 450 nm. These monooxygenases catalyze a dazzling array of regio- and stereospecific oxidation reactions, including the hydroxylation of aliphatic and aromatic hydrocarbons and the epoxidation of alkenes (1, 2). P450s take two reducing equivalents from NAD(P)H and deliver one atom from dioxygen to the organic substrate; the other oxygen atom is released as water. The consensus mechanism for P450 catalysis (Fig. 1) implicates a ferryl porphyrin radical cation [compound I (**CI**): Fig. 1, intermediate **6**] as the active oxygenating agent (3), but this elusive species has not been observed in P450 under single-turnover or steady-state catalytic conditions. In the postulated mechanism, **CI** is proposed to abstract a hydrogen atom from the substrate to form transient Fe^{IV}-hydroxide complex (compound II, **CII**), followed by radical recombination to produce oxygenated product (4, 5). Mechanistic studies of P450 catalysis in cryogenic matrices have suggested that the barrier to formation of **CI** ($5 \rightarrow 6$) is higher than that for its reaction with substrate ($6 \rightarrow 7 \rightarrow 1$) (6). Consequently, recent efforts have focused on alternate routes to P450 **CI** that bypass the hydroperoxide intermediate (**5**). One approach employs generation of **CII** using peroxynitrite, followed by laser flash photolysis to yield **CI** (7). This technique has been used in studies of the spectra and reactivity of the putative **CI** species, but the interpretation of the results remains open to question.

In earlier work, we employed $[Ru(bpy)_3]^{2+}$ (bpy = 2,2′-bipyridine) in a bimolecular flash-quench photochemical oxidation protocol to generate **CII** and **CI** in horseradish peroxidase (HRP) and the heme octapeptide from cytochrome *c* (MP8) (8, 9). This approach was unsuccessful with P450, however, owing to the deep burial of the heme inside the polypeptide matrix of the enzyme. We have circumvented this problem by covalently attaching a ruthenium-diimine photosensitizer to a nonnative cysteine residue on the P450 surface.

The structurally characterized soluble heme domain of P450-BM3 from *Bacillus megaterium* serves as a model for the
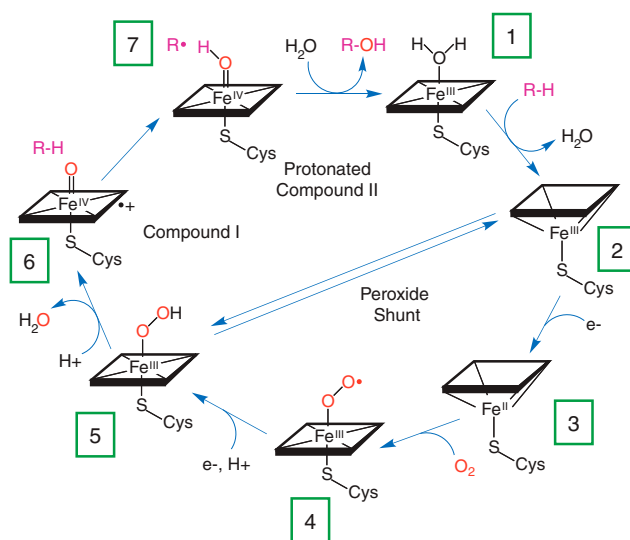

Fig. 1. Schematic representation of the consensus P450 catalytic cycle and peroxide shunt pathway.

mammalian proteins (10). To ensure a unique attachment of the ruthenium-diimine photosensitizer to the P450, we have used site-directed mutagenesis to remove two native cysteine residues (C62A, C156S) and replace a surface lysine with cysteine at position 97 (K97C); this triple mutant has been overexpressed in *Escherichia coli*. The complex $[Ru(bpy)_2(IA-phen)]^{2+}$ (IA-phen = 5-iodoacetamido-1,10-phenanthroline) was covalently coupled to Cys97 to give the conjugate Ru^{II}_{K97C}-Fe^{III}_{P450}. This conjugate was characterized by mass spectrometry, UV-visible and luminescence spectroscopies, and X-ray crystallography. In our laser flash-quench experiments, this species undergoes rapid photooxidation of the resting ferric-aquo complex to form **CII**.

Results and Discussion

X-Ray Crystal Structure Analysis We have determined the X-ray crystal structure of Ru^{II}_{K97C}-Fe^{III}_{P450} to a resolution of 2.4 Å (Table S1). Two monomers were found in the asymmetric unit; the rmsd between the C_α atom positions in the two monomers is 0.34 Å, confirming that the two polypeptides have nearly identical conformations. The structure of Ru^{II}_{K97C}-Fe^{III}_{P450} more

Fig. 2. Ru^{II}_{K97C}-Fe^{III}_{P450} heme region based on an X-ray crystal structure analysis showing covalent attachment of $[Ru(bpy)_2(A\text{-phen})]^{2+}$ at the nonnative cysteine residue (C97) with $d(Ru\text{-}Fe) = 24$ Å and the hydrogen bonding interaction between the tryptophan residue at position 96 and one of the propionics.

closely resembles that of the substrate-bound P450-BM3 enzyme (rmsd of 0.5 Å for the structure 2UWH; ref. 11) than the substrate-free protein (rmsd of 1.3 Å for the structure 2BMH; ref. 12). Interestingly, the substrate channel is occupied by two unidentified electron density peaks; the Ru^{II}_{K97C}-Fe^{III}_{P450} structure likely represents the substrate-bound conformational state. The Ru-photosensitizer is well defined only in one monomer of the crystal structure, owing to π-stacking of the bipyridine ligands with aromatic residues on adjacent crystal units. The Fe-Ru distance between the heme and Ru-photosensitizer is 24 Å (Fig. 2). The Ru-photosensitizer in the second monomer, which lacks the π-stacking interactions with neighboring protein molecules, is highly disordered, possibly due to flexibility of the cysteine-acetamide linkage. These observations indicate a degree of conformational freedom for the Ru-photosensitizer. The 24-Å Ru-Fe distance is likely near the maximum separation in the distribution of conformations sampled by the Ru complex in dilute Ru^{II}_{K97C}-Fe^{III}_{P450} solutions since the ligands of the photosensitizer may form favorable hydrophobic or π-stacking interactions with amino acid residues on the protein surface, decreasing the Fe-Ru separation.

Laser Flash-Quench Experiments As expected, the Ru-diimine sensitizer in Ru^{II}_{K97C}-Fe^{III}_{P450} luminesces upon 480-nm excitation: The spectrum closely resembles those of $[Ru(bpy)_2(IA\text{-phen})]^{2+}$ and $[Ru(bpy)_3]^{2+}$. The luminescence decay in Ru^{II}_{K97C}-Fe^{III}_{P450} ($\lambda_{obsd} = 630$ nm) is biexponential, whereas $\tau(*[Ru(bpy)_2(IA\text{-phen})]^{2+}$ is monoexponential [τ_1 ($*Ru^{II}_{K97C}$-Fe^{III}_{P450}) = 670 ns, τ_2 ($*Ru^{II}_{K97C}$-Fe^{III}_{P450}) = 140 ns; $\tau(*[Ru(bpy)_2(IA\text{-phen})]^{2+}$) = 720 ns], possibly due to multiple conformations of the tethered photosensitizer (Fig. S1). Stern–Volmer analysis

of $*Ru^{II}_{K97C}$-Fe^{III}_{P450} luminescence decay in the presence of an exogenous electron-transfer quencher ($[Ru(NH_3)_6]^{3+}$) produces a quenching rate constant (k_q) of 1.4×10^9 M^{-1} s^{-1} (Fig. S2).

We used transient absorption (TA) spectroscopy to characterize the intermediates formed following excitation of Ru^{II}_{K97C}-Fe^{III}_{P450}; measurements in the heme Soret region (390–440 nm) provide the largest TA signals. The Ru-diimine complex also contributes substantially to absorbance in this region, enabling us to monitor changes in both photosensitizer and heme oxidation states (Fig. S3). TA traces of Ru^{II}_{K97C}-Fe^{III}_{P450} following excitation in the absence of exogenous quencher (pH 8, $\lambda_{ex} = 480$ nm, 10 ns pulse) reveals bleaching ($\Delta Abs < 0$) at wavelengths corresponding to Ru^{II} absorption (390–440 nm), consistent with the well-characterized behavior of metal-to-ligand charge-transfer (MLCT) excited Ru-diimine complexes (13). The transient signal returns to baseline at the same rate as luminescence decays and we find no evidence for transient species associated with changes in heme Soret absorption.

In the presence of quencher (17 mM $[Ru(NH_3)_6]^{3+}$), the TA kinetics become substantially more complex, revealing the presence of multiple intermediates that form and disappear over the microsecond to second time range (Fig. 3). A generalized singular value decomposition analysis of the data (14) indicates that as many as five distinct kinetics phases contribute to the recovery of the TA signal (Fig. S4). Global least-squares fitting of the TA data recorded at six different wavelengths to a sum of five exponentials with amplitude coefficients ρ_{1-5} produces the observed rate constants γ_{1-5} listed in Table 1. We find analogous trends in the TA data recorded at pH 6 and 7.

Flash-Quench Electron Transfer The five distinct phases observed in the TA data suggest that six distinct species are formed following excitation of the Ru photosensitizer. The first transient species is easily identified as $*Ru^{II}_{K97C}$-Fe^{III}_{P450}, and the second, Ru^{III}_{K97C}-Fe^{III}_{P450}, is formed in the quenching reaction with $[Ru(NH_3)_6]^{3+}$. The final species formed is Ru^{II}_{K97C}-Fe^{III}_{P450}, because all TA signals return to baseline. Three transient species remain to be identified; we anticipate that these are associated with oxidation of the P450 heme center (P450$_{OX1-3}$) (Scheme 1).

In our studies of flash-quench **CII** generation in HRP and MP8, we found that ferryl-heme formation was preceded by a porphyrin oxidation step; subsequent internal rearrangement and deprotonation led to the $Fe^{IV}(O)P$ product. Based on this reasoning, we have developed a sequential kinetics model for the Ru^{II}_{K97C}-Fe^{III}_{P450} TA data (Fig. 4). We have solved the rate law for this model, allowing us to express the observed rate constants (γ_{1-5}) and amplitude coefficients (ρ_{1-5}) in terms of nine elementary rate constants ($k_0, k_1, k_2, k_3, k_4, k_5, k_6, k_{-6}, k_7$) and the initial $*Ru^{II}_{K97C}$-Fe^{III}_{P450} concentration.

The parameters in the kinetics model cannot be determined by the data alone: Values for k_1, k_3, k_5, and $K_{eq} = k_6/k_{-6}$ must be supplied in order to determine absolute molar difference spectra for the six intermediate species. The known spectra of $*Ru^{II}$- and
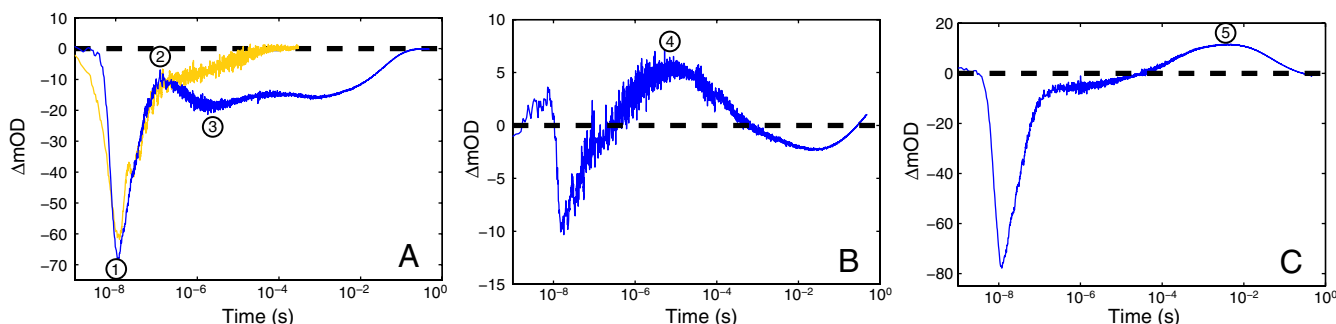
Fig. 3. Single-wavelength transient absorption kinetics for Ru^{II}_{K97C}-Fe^{III}_{P450} with quencher, pH 8. Circled numbers correspond to the beginning of each phase: (*A*) 420 nm Ru^{II}_{K97C}-Fe^{III}_{P450} (blue) and $[Ru(bpy)_2(IA\text{-phen})]^{2+}$ (yellow); (*B*) 390 nm; (*C*) 440 nm.

pH	γ_1, s^{-1}	γ_2, s^{-1}	γ_3, s^{-1}	γ_4, s^{-1}	γ_5, s^{-1}
6	$2.5(3) \times 10^7$	$1.5(5) \times 10^6$	$2.0(3) \times 10^5$	$2(1) \times 10^4$	$6(1) \times 10^1$
7	$2.4(3) \times 10^7$	$1.5(6) \times 10^6$	$1.5(3) \times 10^5$	$1.2(3) \times 10^4$	$7(2) \times 10^1$
8	$3.0(4) \times 10^7$	$2(5) \times 10^6$	$1.0(3) \times 10^5$	$4(1) \times 10^3$	$3(1) \times 10^1$

Data from six different wavelengths were fit to the following function: $\Delta Abs(\lambda, t) = \rho_1(\lambda) \exp(-\gamma_1 t) + \rho_2(\lambda) \exp(-\gamma_2 t) + \rho_3(\lambda) \exp(-\gamma_3 t) + \rho_4(\lambda) \exp(-\gamma_4 t) + \rho_5(\lambda) \exp(-\gamma_5 t)$. The rate constant γ_1 was fixed to the value obtained from single-exponential fits to the luminescence decay kinetics.

Ru^{III}-diimine constrain the possible values of k_1 and k_3. The balance between k_5 and k_7 has no effect on the relative difference spectra extracted from the data, so k_5 was set equal to k_7. The equilibrium constant K_{eq} was optimized to provide the best agreement between the transient difference spectra recorded at the three different pH values (Fig. 5).

The difference spectra of $^*Ru^{II}_{K97C}$-Fe^{III}_{P450} and Ru^{III}_{K97C}-Fe^{III}_{P450} extracted from the kinetics analysis exhibit bleaching at 430 nm of the Ru^{II} MLCT absorption band (Fig. S5). Of primary interest are the difference spectra corresponding to intermediates $P450_{OX1-3}$ (Fig. S5). The spectra of $P450_{OX1}$ and $P450_{OX2}$ are quite similar, characterized by a bleach of the Soret absorption band (centered at 420 nm). The spectrum of $P450_{OX2}$ displays somewhat more absorbance at 390 nm than that of $P450_{OX1}$ but otherwise closely resembles that of $P450_{OX1}$. Reasoning by analogy to our results on the oxidation of HRP and MP8, and the similarity of their difference spectra, we suggest that $P450_{OX1}$ and $P450_{OX2}$ correspond to porphyrin radical cations: Ru^{II}_{K97C}-$Fe^{III}(OH_2)P^{\bullet+}_{(A)P450}$ and Ru^{II}_{K97C}-$Fe^{III}(OH_2)P^{\bullet+}_{(B)P450}$. These difference spectra are consistent with the difference spectrum of CPO CI, which is characterized as an $Fe^{IV}(O)P^{\bullet+}$ center (15). Flash-quench-triggered oxidation of HRP and MP8 produces a similarly bleached, six-coordinate ferric porphyrin radical cation ($Fe^{III}P^{\bullet+}$) (8). The blue shift in absorption for these porphyrin radical intermediates is also consistent with synthetic models of Fe(III)-porphyrin cation radicals (16).

The specific rate of $Fe^{III}(OH_2)P^{\bullet+}_{(A)P450}$ formation in our conjugate (Table S2) is comparable to that found for reconstituted myoglobin containing a heme tethered directly to $Ru(bpy)_3^{2+}$ (17). This observation suggests that a favorable pathway couples the P450 porphyrin to Ru^{III}, possibly involving the Trp96-heme propionate hydrogen bond (18). The conversion of Ru^{II}_{K97C}-$Fe^{III}(OH_2)P^{\bullet+}_{(A)P450}$ to Ru^{II}_{K97C}-$Fe^{III}(OH_2)P^{\bullet+}_{(B)P450}$ may be a consequence of changes in polypeptide or solvent conformation in the P450 heme pocket (19).

The apparent equilibrium constant between $P450_{OX2}$ and $P450_{OX3}$ varies with pH (K_{eq}: 0.8, pH 6; 2.9, pH 7; 10, pH 8) suggesting that a proton is lost in the formation of $P450_{OX3}$. Moreover, the difference spectrum for this species indicates a red-shifted Soret absorption band analogous to that reported for the $Fe^{IV}(OH)P$ center in CPO CII (20). Hence, we suggest that $P450_{OX3}$ is Ru^{II}_{K97C}-$Fe^{IV}(OH)P_{P450}$. Internal charge transfer in $Fe^{III}(OH_2)P^{\bullet+}_{(B)P450}$ is accompanied by rapid loss of a proton (possibly to water), producing $Fe^{IV}(OH)P_{P450}$. On the basis of results for HRP and MP8, we expect this heme rearrangement to be pH dependent. The formation of flash-quench-generated CII in HRP was slower (k_{obs} of 4.1 s^{-1}) due to rate-limiting water ligation. CII formation in P450 proceeds on the millisecond timescale because the sixth coordination site of the ferric heme is occupied by a water molecule.

All of these intermediates are short-lived; transient absorbances return to baseline within 500 ms, indicating recovery of Ru^{II}_{K97C}-$Fe^{III}(OH_2)P_{P450}$. We have modeled this process as recovery from both the ferryl species [k_7, Ru^{II}_{K97C}-$Fe^{IV}(OH)P_{P450}$] and its porphyrin radical cation precursor [k_5, Ru^{II}_{K97C}-$Fe^{III}(OH_2)P^{\bullet+}_{(B)P450}$] (Fig. 4), but it is not possible to determine the two rate constants because equilibration between Ru^{II}_{K97C}-$Fe^{III}(OH_2)P^{\bullet+}_{(B)P450}$ and Ru^{II}_{K97C}-$Fe^{IV}(OH)P_{P450}$ is faster than the ground-state recovery process. The precise nature of the ground-state recovery process remains unclear. It should be described by second-order reaction kinetics, but the experimental data are modeled better by a simple exponential process. Nevertheless, $[Ru(NH_3)_6]^{2+}$ seems to be involved in the recovery reaction because, in the presence of $[Ru(NH_3)_6]^{3+}$ as quencher, transient absorption data are consistent over the course of multiple hours, and the Soret absorption band appears relatively unaffected after many rounds of flash-quench excitation. However, similar measurements with an irreversible quencher ($[Co(NH_3)_5Cl]^{3+}$) induces bleaching of the Soret band and rapid sample degradation.

## Concluding Remarks

We have developed a flash-quench method to oxidize the buried resting state ferric-aquo compound of the P450-BM3 heme domain to CII without the use of reactive oxygen species (O_2, H_2O_2). The catalytic cycle runs in reverse by photochemically splitting water at the heme site. It is likely that the observed ferryl species is protonated over a pH range of 6–8, as consistent with the current view of chloroperoxidase and P450 CII. The finding that internal oxidation of the iron center is rate limiting has allowed us to observe porphyrin radical cation intermediates. As porphyrin oxidation occurs on the microsecond timescale, we can reasonably expect a second round of flash-quench on photochemically generated CII to produce CI.

Materials and Methods

Protein Expression. A plasmid containing the C62A/C156S double mutant of the P450-BM3 heme domain in the vector pCWori$^+$ was obtained courtesy of Andrew Udit (Occidental College, Los Angeles, CA). A cysteine residue for photosensitizer coupling was introduced at residue 97 using a QuikChange Site-Directed Mutagenesis kit (Qiagen). All primers were purchased from Operon. Mutant cytochromes were expressed with an N-terminal His$_6$ tag in Escherichia coli BL21(DE3) cells and purified according to literature procedure (21). Proteins were characterized by SDS-PAGE and MS analysis.

Photosensitizer Synthesis and Coupling to P450-BM3. Ruthenium(II) bisbipyridine 5-acetamido-1,10-phenanthroline ($[Ru(bpy)_2(IA-phen)]^{2+}$) was synthesized according to the published procedure (22) with the following modification: In lieu of final precipitation as the PF$_6$ salt, the compound was redissolved in water without further purification. Approximately twofold excess of $[Ru(bpy)_2(IA-phen)]^{2+}$ was added to a 20 μM solution of C62A/C156S/K97C P450-BM3 in 20 mM Tris buffer (pH 8), and shaken in the dark at 4 °C. Labeling progress was monitored by MALDI mass spectro-
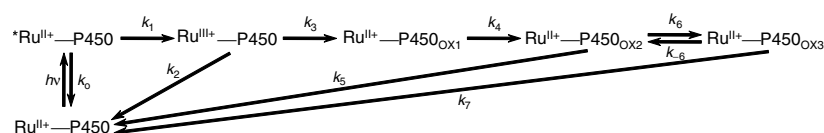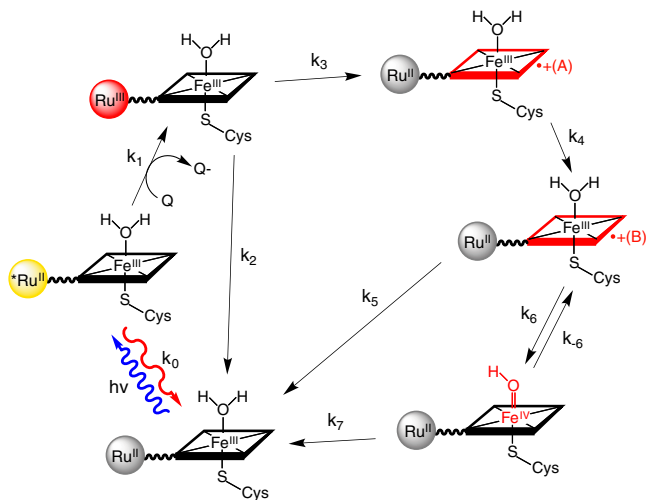

Scheme 1.

Fig. 4. Diagram of the model for photochemical heme oxidation in Ru_{K97C}-Fe^{III}_{P450} used in the analysis of transient absorption kinetics data.

metry; no further increase in the peak at 54.2 kDa (corresponding to the predicted mass of Ru^{II}_{K97C}-Fe^{III}_{P450}) was observed after 2 h. Excess $[Ru(bpy)_2(IA\text{-}phen)]^{2+}$ was removed during concentration in 30 kDa filters, followed by desalting on an FPLC HiPrep column. Photosensitizer-labeled (Ru^{II}_{K97C}-Fe^{III}_{P450}) and unlabeled proteins were separated using an anion exchange MonoQ column. The labeled protein was characterized by CO binding, and purity was confirmed by SDS-PAGE and mass spectrometry. The conjugate Ru^{II}_{K97C}-Fe^{III}_{P450} demonstrated activity in the hydroxylation of lauric acid via the peroxide shunt (21).

Crystal Structure Determination. Crystals of Ru^{II}_{K97C}-Fe^{III}_{P450} were obtained by the sitting-drop vapor diffusion method: 27 mg/mL Ru^{II}_{K97C}-Fe^{III}_{P450} in 10 mM potassium phosphate, pH 8.4, were mixed with a crystallization well solution of 2 M $(NH_4)_2SO_4$ (wt/vol) in a 1:1 ratio (vol/vol). Crystals formed over a period of 2 d at 4 °C, and were flash-frozen directly from the crystallization solution. X-ray diffraction data were collected at 100 K using beamline 7-1 at the Stanford Synchrotron Radiation Laboratory. Detailed description of the structure determination is provided in the *SI Text*. Statistics for data collection and refinement are shown in Table S1. Atomic coordinates and structure factors were deposited in the Protein Data Bank under the entry 3NPL.

Laser Flash-Quench. Samples consisting of $[Ru(bpy)_2(IA\text{-}phen)]^{2+}$ or Ru^{II}_{K97C}-Fe_{P450} (~10 μM) with and without quencher (17 mM ruthenium(III)-hexaammine trichloride) were prepared in buffered solution (pH 6, 20 mM sodium acetate; pH 7, 20 mM sodium acetate; pH 8, 50 mM sodium borate or 50 mM
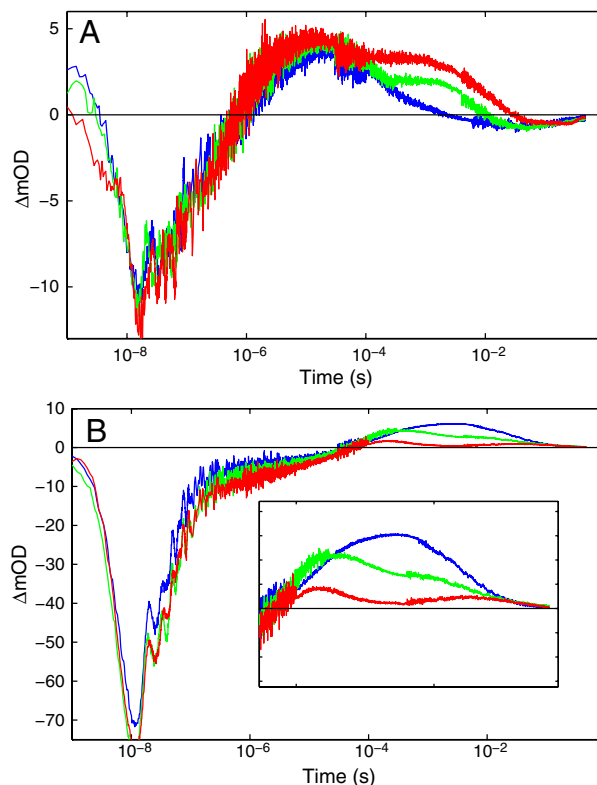

Fig. 5. Dependence of transient absorption kinetics on pH (red, pH 6; green, 7; blue, 8): (*A*) 390 nm, (*B*) 440 nm.

Tris). Deoxygenation was achieved via 30 gentle pump-backfill cycles with argon. Samples were excited with 10 ns laser pulses at 480 nm, delivered by an optical parametric oscillator pumped by the third harmonic from a Spectra Physics Q-switched Nd:YAG laser. Luminescence decays were monitored at 630 nm. Single wavelength TA kinetics were monitored every 10 nm from 390–440 nm, averaging ~500 shots per wavelength. Data from five separate timescales (2 μs, 40 μs, 400 μs, 10 ms, and 500 ms) were collected and spliced together to produce full kinetics traces.

1. Guengerich FP (2001) Common and uncommon cytochrome P450 reactions related to metabolism and chemical toxicity. *Chem Res Toxicol* 14:611–650.
2. Ortiz de Montellano P (2005) *Cytochrome P450: Structure, Mechanism and Biochemistry* (Kluwer/Plenum, New York), 3rd Ed, p 689.
3. Denisov IG, Makris TM, Sligar SG, Schlichting I (2005) Structure and chemistry of cytochrome P450. *Chem Rev* 105:2253–2278.
4. Groves JT (2003) The bioinorganic chemistry of iron in oxygenases and supramolecular assemblies. *Proc Natl Acad Sci USA* 100:3569–3574.
5. Green MT (2009) C-H bond activation in heme proteins: The role of thiolate ligation in cytochrome P450. *Curr Opin Chem Biol* 13:84–88.
6. Davydov R, et al. (2001) Hydroxylation of camphor by reduced oxy-cytochrome P450cam: Mechanistic implications of EPR and ENDOR studies of catalytic intermediates in native and mutant enzymes. *J Am Chem Soc* 123:1403–1415.
7. Wang Q, Sheng X, Horner JH, Newcomb M (2009) Quantitative production of compound I from a cytochrome P450 enzyme at low temperatures. Kinetics, activation parameters, and kinetic isotope effects for oxidation of benzyl alcohol. *J Am Chem Soc* 131:10629–10636.
8. Berglund J, Pascher T, Winkler JR, Gray HB (1997) Photoinduced oxidation of horseradish peroxidase. *J Am Chem Soc* 119:2464–2469.
9. Low D, Winkler J, Gray H (1996) Photoinduced oxidation of microperoxidase-8: Generation of ferryl and cation-radical porphyrins. *J Am Chem Soc* 118:117–120.
10. Munro AW, et al. (2002) P450 BM3: The very model of a model flavocytochrome. *Trends Biochem Sci* 27:250–255.
11. Huang W, et al. (2007) Filling a hole in cytochrome P450 BM3 improves substrate binding and catalytic efficiency. *J Mol Biol* 373:633–651.
12. Li H, Poulos T (1995) Modeling protein-substrate interactions in the heme domain of cytochrome P450(BM-3). *Acta Crystallogr, Sect D: Biol Crystallogr* 51:21–32.
13. Creutz C, Chou M, Netzel TL, Okumura M (1980) Lifetimes, spectra, and quenching of the excited states of polypyridine complexes of iron(II), ruthenium(II), and osmium(II). *J Am Chem Soc* 102:1309–1319.
14. Hansen PC (1994) Regularization tools: A Matlab package for analysis and solution of discrete ill-posed problems. *Numer Algorithms* 6:1–35.
15. Rittle J, Younker JM, Green MT (2010) Cytochrome P450: The active oxidant and its spectrum. *Inorg Chem* 49:3610–3617.
16. Ikezaki A, Tukada H, Nakamura M (2008) Control of electronic structure of a six-coordinate iron(III) porphyrin radical by means of axial ligands. *Chem Commun* 2257–2259.
17. Hamachi I, Tsukiji S, Shinkai S, Oishi S (1999) Direct observation of the ferric-porphyrin cation radical as an intermediate in the phototriggered oxidation of ferric- to ferryl-heme tethered to Ru(bpy)3Ru(bpy)$_3$ in reconstituted materials. *J Am Chem Soc* 121:5500–5506.
18. Shih C, et al. (2008) Tryptophan-accelerated electron flow through proteins. *Science* 320:1760–1762.
19. Fishelovitch D, Shaik S, Wolfson HJ, Nussinov R (2010) How does the reductase help to regulate the catalytic cycle of cytochrome P450 3A4 using the conserved water channel? *J Phys Chem B* 114:5964–5970.
20. Green MT, Dawson JH, Gray HB (2004) Oxoiron(IV) in chloroperoxidase compound II is basic: Implications for P450 chemistry. *Science* 304:1653–1656.
21. Cirino PC, Arnold FH (2002) Regioselectivity and activity of cytochrome P450 BM-3 and mutant F87A in reactions driven by hydrogen peroxide. *Adv Synth Catal* 344:932–937.
22. Castellano FN, Dattelbaum JD, Lakowicz JR (1998) Long-lifetime Ru(II) complexes as labeling reagents for sulfhydryl groups. *Anal Biochem* 255:165–170.